ACS OMEGA

Open Access

This article is licensed under CC-BY-NC-ND 4.0

http://pubs.acs.org/journal/acsodf

Article

Leaching Vanadium from the Spent Denitration Catalyst in the Sulfuric Acid/Oxalic Acid Combined Solvent

Wenting Cheng,* Jie Li, Jianhang Deng, Yang Li,* and Fangqin Cheng

Cite This: *ACS Omega* 2024, 9, 9286−9294

Read Online

ACCESS | Metrics & More | Article Recommendations

ABSTRACT: Huge amounts of spent denitration catalysts are produced annually as waste from the flue gas denitration process, which will cause resource waste and environmental pollution. It is important to develop an efficient method for the recovery of metals from spent denitration catalysts. In this work, the leaching of vanadium (V) from the spent denitration catalyst by the sulfuric acid/oxalic acid combined solvent was investigated. Factors that influence the leaching rate of V have been studied. Results showed that the optimal leaching rate was 95.65% by 20 wt % sulfuric acid and 0.3 mol·L^{-1} oxalic acid with a liquid-to-solid ratio of 20 mL·g^{-1} at 140 °C for 7 h. For further study of the leaching process, the leaching mechanism of V was explored subsequently. Results indicated that sulfuric acid provided a strongly acidic environment, which was beneficial to transformation, complexation, and redox reactions of V in the mixed acid leaching system. Meanwhile, oxalic acid with excellent complexation and reducing−dissolving properties promoted the formation of stable water-soluble VO^{2+}. The "complex effect" generated from the combined acids was greatly favored for leaching V from the spent denitration catalyst.

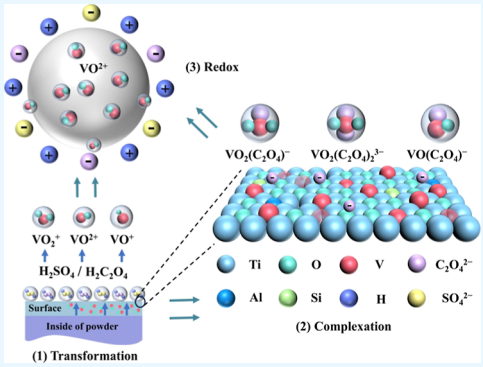

1. INTRODUCTION

The selective catalytic reduction (SCR) flue gas denitration technology is widely used in coal-fired power plants for its high efficiency, reliable operation, no secondary pollution, etc.[1,2] As the core of the SCR denitration system, the catalytic activity of the V/Ti catalyst is directly related to the denitration effect.[3] However, the catalytic activity of the catalyst will gradually diminish with the extension of operating time in the complex flue gas systems, and its service life is only 3−4 years generally.[4] About 60% of the catalyst have no regeneration value due to their damaged physical structure or decreased mechanical properties, which typically will be landfilled.[5] This has caused not only the waste of national strategic reserve metals, such as vanadium (V), tungsten (W), and titanium (Ti), but also a severe environmental risk.[6] Therefore, it is of great importance to realize the extraction of these valuable metals from spent denitration catalysts.[7,8]

Numerous studies on the extraction and purification of V from spent denitration catalysts have been carried out.[9,10] Currently, the common methods for extraction V from spent denitration catalysts include alkaline leaching,[11] sodium roasting,[12] and single-acid leaching.[13] Among these methods, alkaline leaching is known for its high alkali consumption and wastewater generation, while sodium roasting causes high energy consumption.[14] The single-acid leaching method, on the other hand, could be further classified into inorganic acid leaching and organic acid leaching.[15,16] Sulfuric acid leaching, one of the inorganic acid leaching methods, is often used in industries due to its mature process and low-grade raw material requirement.[17] In this method, high concentrations of sulfuric acid are required to achieve a high leaching rate of V. Thus, this process inevitably discharges large amounts of sulfuric leachate after ion exchange, causing serious environmental pollution.[7] Additionally, the leaching rate of V will reduce significantly with a decrease of the concentration of sulfuric acid. For example, the leaching rate of V reduces sharply from 80 to 47% as the concentration of sulfuric acid decreases from 6.0 to 1.0 mol·L^{-1}.[18] This case might be possible because the reduction of the acidity in the leaching system would lead to the hydrolysis of the leached V.[19] These problems reflect the limitation of using sulfuric acid as a single leaching agent for V leaching. Therefore, developing new methods for efficiently extracting V from spent denitration catalysts is practical and economic for the sustainable development of the catalyst industry.

Oxalic acid is one of the most promising organic acids acting as both leaching and reducing reagents.[10] It has been intensively applied for metal extraction such as Fe, V, W, etc.

Received: October 26, 2023
Revised: January 26, 2024
Accepted: January 26, 2024
Published: February 16, 2024

© 2024 The Authors. Published by American Chemical Society

from minerals or secondary resources.[20] For example, Hu et al.[21] reported that 71.6% of the V was extracted by 6.0 mol·kg^{-1} oxalic acid with a leaching time of 4 h at 95 °C. Wu et al.[22] also found that 84% of V could be leaching by 1.0 mol·L^{-1} oxalic acid at 90 °C. Compared with sulfuric acid, oxalic acid has better environmental adaptability but a higher price.[23] Moreover, the acidity of oxalic acid is weaker than that of sulfuric acid at the same concentration.[24] To efficiently leach metals and achieve the economic and environmental goals of the industry, an inorganic acid and organic acid mixture was used as a leaching solvent.[25] For instance, Wang and Yang.[26] leached V from the spent SCR catalyst by sulfuric acid−ascorbic acid with a leaching rate of 96.25%. Li et al.[27] extracted metals from spent lithium-ion batteries using a sulfuric acid−malonic acid mixture. The results showed that 99.46% Ni, 97.24% Co, and 96.88% Mn were extracted under optimal conditions. However, leaching V from the spent denitration catalyst using the sulfuric acid/oxalic acid mixture as leaching solvents was rarely reported. Moreover, more attention should be given to the leaching mechanism of V in the sulfuric acid/oxalic acid combined solvent as it plays an important role for improving the leaching rate of V from the spent denitration catalyst.

In this work, the leaching of V from the spent denitration catalyst was conducted with sulfuric acid/oxalic acid combined solvent. Liquid-to-solid (L/S) ratio, concentrations of sulfuric acid and oxalic acid, reaction temperature, and leaching time were investigated as key factors to determine the optimum leaching condition. The leaching rate, mineral phase transformation, and valence change of V during the leaching process were investigated by scanning electron microscopy (SEM), energy-dispersive X-ray spectroscopy (EDS), X-ray photoelectron spectroscopy (XPS), inductively coupled plasma optical emission spectrometry (ICP−OES), X-ray diffraction (XRD), Fourier transform infrared (FTIR) spectra, and UV−vis analysis. Eventually, the leaching mechanism of V in the sulfuric acid/oxalic acid combined system was investigated based on the kinetics analysis.

2. EXPERIMENTAL SECTION

2.1. Materials. The spent denitration catalyst was collected from Jiangsu Longking−Coalogix Environmental Protection Technology Co., Ltd., China. The collected sample was dried at 80 °C for 24 h and ground to obtain powdered samples with a size smaller than 75 μm. It was then stored in an airtight container. The particle size of the spent denitration catalyst could strongly affect the leaching rate of the metals from it.[28] Therefore, all the leaching experiments were conducted using spent denitration catalyst particles with a size smaller than 75 μm to avoid the decrease of the leaching rate.[29]

Sulfuric acid (H_2SO_4, 98.0%), oxalic acid ($H_2C_2O_4{\cdot}2H_2O$, 99.8%), vanadyl sulfate ($VOSO_4$, 99.9%), and vanadyl oxalate ($VOC_2O_4{\cdot}5H_2O$, 98.5%) were purchased from Sinopharm Chemical Reagents Co., Ltd., China. The water used in this work for solution preparation, dilution, sample washing, etc. was double distilled water (conductivity <0.1 μS·cm^{-1}).

2.2. Characteristics. The elemental composition analysis of the spent denitration catalyst was performed by using X-ray fluorescence (XRF, S8 TIGER, Brook Ax, Germany). Morphological and elemental analyses of the spent denitration catalyst were performed using a scanning electron microscope equipped with an energy-dispersive X-ray spectroscope (SEM−EDS, JSM−IT500HR, Sharp Corporation, Japan). The chemical form of V, W, and Ti in the spent denitration catalyst was determined through XPS (ESCALAB 250 Xi, Thermo Fisher Scientific, America). The concentrations of elements in the leaching solution were analyzed by using ICP−OES (Optima 5800VD, Agilent, America). The composition of the solid phases was identified using XRD (SmartLab, Rigaku Corporation, Japan). The FTIR spectra of the spent denitration catalyst was recorded using a Bruker instrument (FTIR, INVENIO−S, Bruker Corporation, Germany). The final valence state of V in the leaching system was determined by using UV−vis spectrophotometry (UV 2600, Shimadzu, China).

2.3. Experimental Procedure. The experimental flowchart is shown in Figure 1. The leaching experiment was performed in a 100 mL homogeneous reactor. A standard volume of the sulfuric acid/oxalic acid combined solvent with a certain concentration was poured into the reactor. The reactor was then electrically stirred and heated. When the solution attained the required temperature (90−150 °C), a certain amount of the spent denitration catalyst was added and kept stirring for 1−9 h. The stirring rate of 500 rpm was selected to eliminate the effect of external diffusion on the leaching process.[28] After each experiment, the slurry was filtered, and the residue was washed three times with distilled water. The leach liquor along with washing water was analyzed for elements using ICP. The leaching rate was calculated according to eq 1

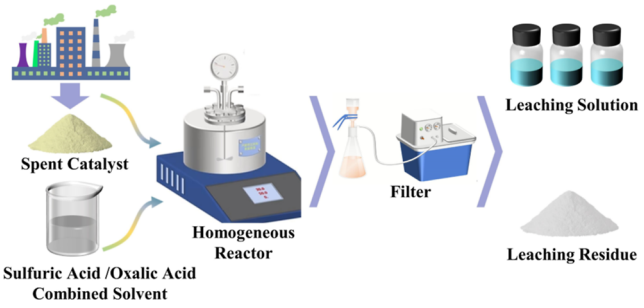

Figure 1. Flowchart of V leaching from spent denitration catalysts.

$$x_i \frac{nVC_i \times 10^{-6}}{mw_i} \times 100\% \quad (1)$$

where x_i was the leaching rate of metals, %; n was the dilution multiple; V was the volume of leaching filtrate, L; C_i was the concentration of metals, mg·L^{-1}; m was the mass of the added spent denitration catalyst, and g; w_i was the content of metals in the spent denitration catalyst, wt %.

3. RESULTS AND DISCUSSION

3.1. Characterization of Spent Denitration Catalysts. The chemical composition of the spent denitration catalyst was analyzed and is listed in Table 1. It can be seen that the main contents of the spent denitration catalyst were TiO_2, WO_3, V_2O_5, SiO_2, CaO, and Al_2O_3. The corresponding mass fraction was 88.76, 3.49, 1.11, 2.88, 1.03, and 0.75%, respectively. The spent denitration catalyst also contained trace amounts of Mg, Na, and K, with mass fractions below 0.1%.

The SEM−EDS analysis of the spent denitration catalyst is shown in Figure 2. The SEM images present irregular-shaped and rod-shaped morphologies of the raw spent denitration

https://doi.org/10.1021/acsomega.3c08452
ACS Omega 2024, 9, 9286−9294

Table 1. Main Chemical Analysis of Spent Denitration Catalysts

component	TiO_2	WO_3	V_2O_5	SiO_2	CaO	Al_2O_3	MgO	Na_2O	K_2O	others
amount (%)	88.76	3.49	1.11	2.88	1.03	0.75	0.095	0.068	0.027	1.79

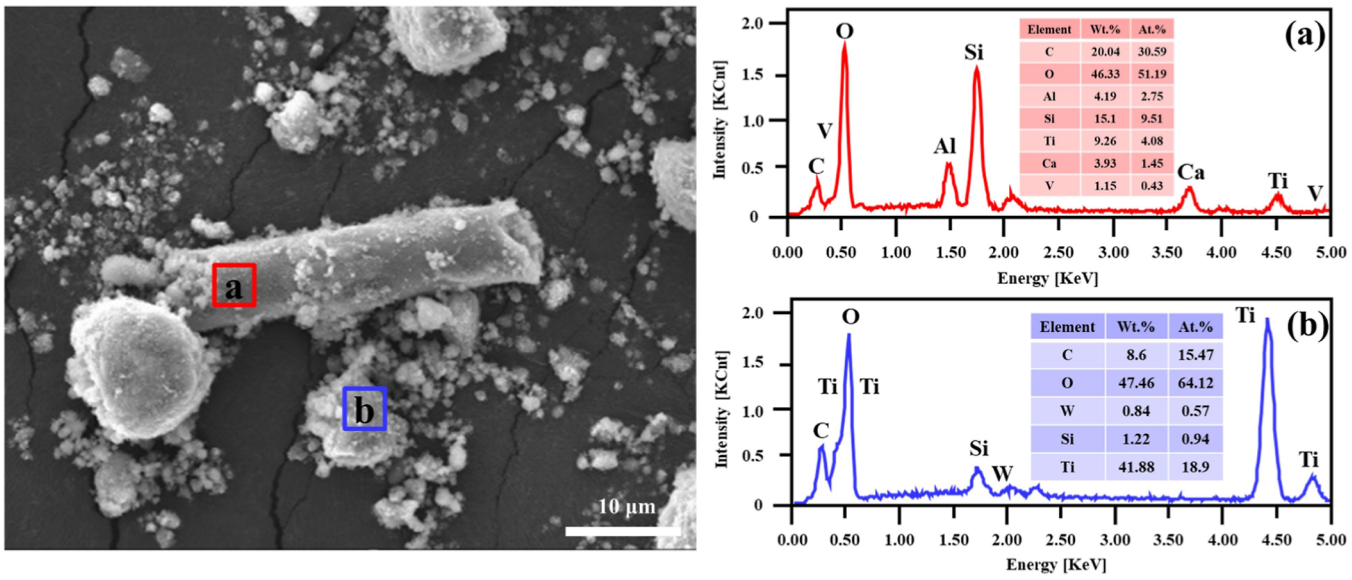

Figure 2. SEM image and EDS spectra of spent denitration catalysts: (a) rod-shaped and (b) irregular-shaped.

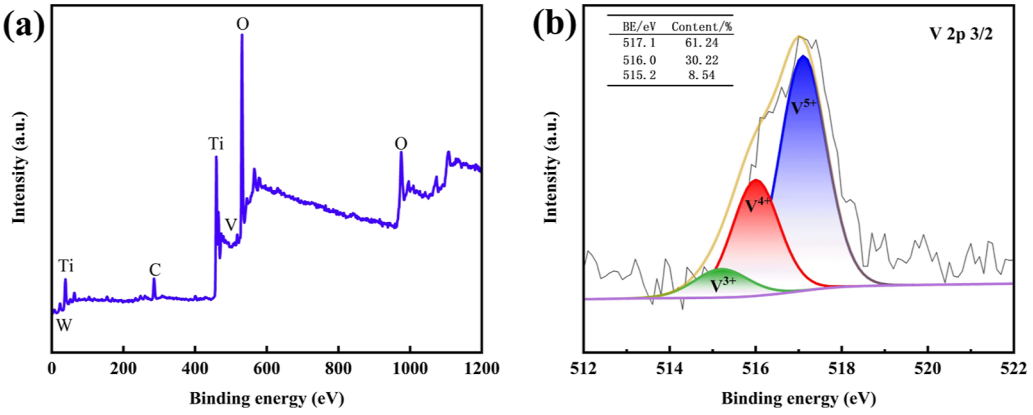

Figure 3. (a) XPS survey spectra and (b) V 2p spectrum of the spent denitration catalyst.

catalyst. The EDS spectra analyses of regions (a) and (b) indicated that the major irregular particles contained W and Ti, whereas rod-shaped particles as binders mainly contained other elements, such as Al, Si, and V. Moreover, the V was encapsulated in the mineral phase with the V-bearing lattice structure (Al−Si−O−V compound) attributed to the prolonged high-temperature sintering during the denitration catalytic process.[30−32] Obviously, only if the V-bearing lattice structure was destroyed by the leaching solvent could ensure a high leaching rate of V.[33]

For further investigating the valence states of element V in the spent denitration catalyst, the element composition analysis was performed by XPS (Figure 3). The C 1s peak at 248.8 eV was used as the internal reference for correcting the binding energy. It could be observed that the primary elements of Ti, W, V, and O along with other minor elements were detected in the spent denitration catalyst (Figure 3a). As shown in Figure 3b, the 2p3/2 spectrum of V had three peaks at 517.1, 516.0, and 515.2 eV, and their corresponding area ratios were 61.24, 30.22, and 8.54%, respectively.[34] The peak at 517.1 eV could be assigned to V^{5+}. The peaks at 516.0 and 515.2 eV could be assigned to V^{4+} and V^{3+}, respectively.[35] Therefore, the V existed in the forms of V_2O_5, V_2O_4, and V_2O_3 in the spent denitration catalyst.[1,22]

3.2. Leaching Analysis of V. The effect of different factors, including L/S ratio, sulfuric acid concentration, oxalic acid concentration, reaction temperature, and leaching time, on the leaching rate of V from the spent denitration catalyst was investigated.

3.2.1. Effect of the L/S Ratio. The effect of L/S ratios (8−22 $mL{\cdot}g^{-1}$) on the leaching rate of V was studied with 30 wt % sulfuric acid and 0.5 $mol{\cdot}L^{-1}$ oxalic acid at 90 °C for 6 h (Figure 4). It could be seen that the leaching rate increased from 75.32 to 82.16% as the L/S ratio from 8 to 20 $mL{\cdot}g^{-1}$ since a higher L/S ratio was beneficial to the mass diffusion between the combined acids and solid particles of the spent denitration catalyst.[22] Moreover, the leaching rate of V was relatively stable when the L/S ratio was further increased from

https://doi.org/10.1021/acsomega.3c08452
ACS Omega 2024, 9, 9286−9294

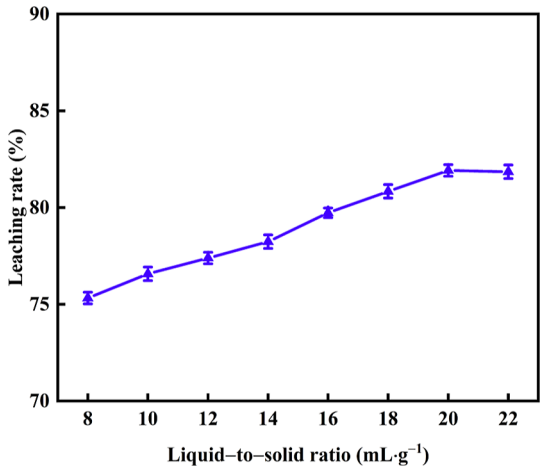

Figure 4. Effect of the L/S ratio on the V leaching rate (conditions: 30 wt % H_2SO_4, 0.5 mol·L^{-1} $H_2C_2O_4$, 90 °C, 6 h).

20 to 22 mL·g^{-1}. It could be seen that there was no use for further improving the leaching rate of V by increasing the L/S ratio when it reached 20 mL·g^{-1}. That was to say the leaching rate of V was saturated under this condition.[27] Therefore, 20 mL·g^{-1} was selected as the best L/S ratio for its corresponding optimal leaching rate of 82.16%.

3.2.2. Effect of the Sulfuric Acid Concentration. The effect of the sulfuric acid concentration (0−30 wt %) on the leaching of V was investigated under the fixed condition: L/S ratio was 20 mL·g^{-1} and 0.5 mol·L^{-1} oxalic acid at 90 °C for 6 h (Figure 5). The leaching rate of V increased from 75.16 to 83.89% as

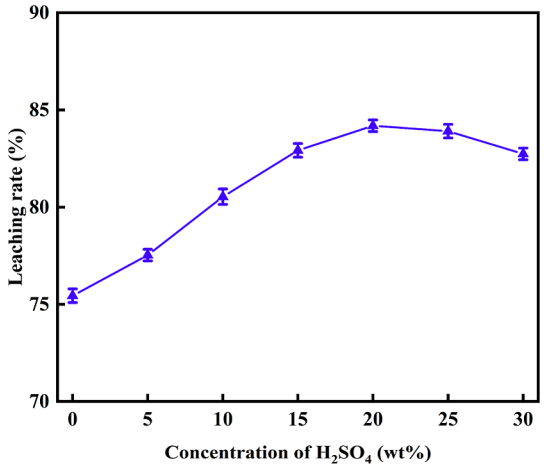

Figure 5. Effect of sulfuric acid on the V leaching rate (conditions: 0.5 mol·L^{-1} $H_2C_2O_4$, 90 °C, 6 h, 20 mL·g^{-1}).

the sulfuric acid concentration increased from 0 to 20 wt % and then decreased to 82.75% as the sulfuric acid concentration increased to 30 wt %. The contact area between sulfuric acid and catalyst particle increased with increasing initial concentration of sulfuric acid (0−20 wt %), thus accelerated the leaching reaction.[27] However, at a higher initial concentration of sulfuric acid (20−30 wt %), the spent denitration catalyst powder had a lower diffusion rate due to the higher viscosity of initial solution, which greatly hindered their release from the solid phase into the liquid phase.[36] Therefore, 20 wt % sulfuric acid concentration was selected for its corresponding optimal leaching rate of 83.89%.

3.2.3. Effect of the Oxalic Acid Concentration. The effect of the oxalic acid concentration (0.3−1.3 mol·L^{-1}) on the leaching of V was studied at an L/S ratio of 20 mL·g^{-1} and 20 wt % sulfuric acid at 90 °C for 6 h (Figure 6). It could be seen

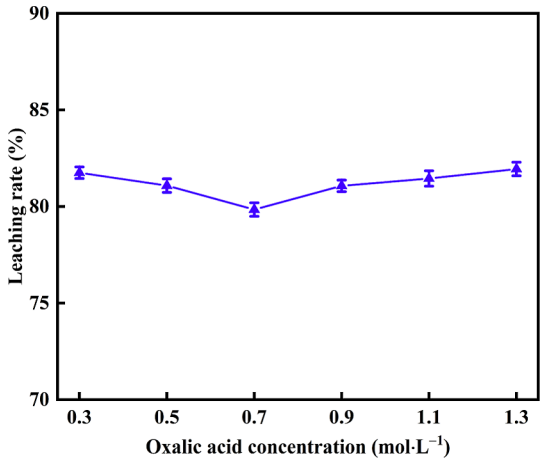

Figure 6. Effect of oxalic acid on the V leaching rate (conditions: 90 °C, 6 h, 20 wt % H_2SO_4, 20 mL·g^{-1}).

that the leaching rate of V initially decreased from 82.75 to 79.84% and subsequently increased to 82.94% with increasing oxalic acid concentration. However, when the concentration of oxalic acid increased to 1.3 mol·L^{-1}, the leaching rate of V was only slightly higher than that of 0.3 mol·L^{-1}. By considering the economy and energy consumption, 0.3 mol·L^{-1} oxalic acid was selected for its corresponding optimal leaching rate of 82.75%.

3.2.4. Effect of Reaction Temperature. The effect of reaction temperature (90−150 °C) on the leaching rate of V was illustrated under a L/S ratio of 20 mL·g^{-1} with 20 wt % sulfuric acid and 0.3 mol·L^{-1} oxalic acid for 6 h (Figure 7). It

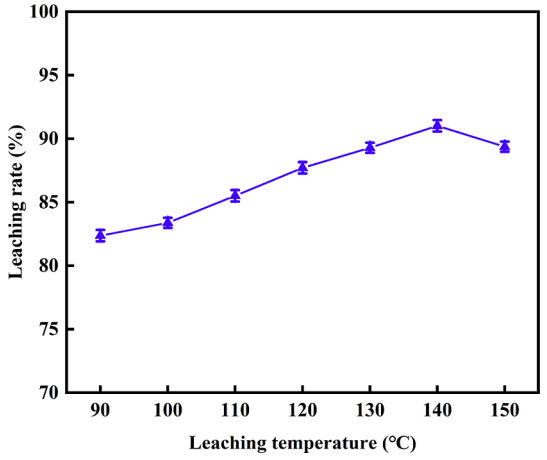

Figure 7. Effect of reaction temperature on the V leaching rate (conditions: 6 h, 0.3 mol·L^{-1} $H_2C_2O_4$, 20 wt % H_2SO_4, 20 mL·g^{-1}).

was indicated that the leaching rate of V significantly increased as the temperature increased from 90 to 140 °C. This case might be attributed to the continued enhancement of the molecular collision.[37] However, the leaching rate of V decreased from 90.02 to 87.54% with further increasing the temperature from 140 to 150 °C. This case might be possible because higher temperature led to the generation of H_2WO_4,

https://doi.org/10.1021/acsomega.3c08452
ACS Omega 2024, 9, 9286−9294

which could cover the surface of the spent denitration catalyst and prevent the leaching of V.[27] Therefore, 140 °C was determined as the optimized reaction temperature for its corresponding optimal leaching rate of 90.02%.

3.2.5. Effect of Leaching Time. The effect of leaching time (3−9 h) on the V leaching rate was depicted under the following conditions: L/S ratio of 20 mL·g^{-1}, 20 wt % sulfuric acid, and 0.3·mol L^{-1} oxalic acid at 140 °C (Figure 8). The

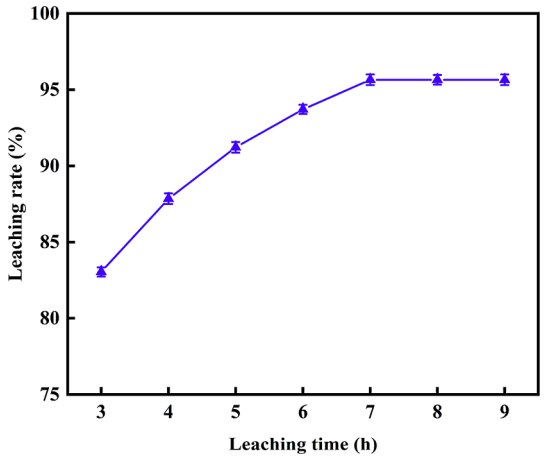

Figure 8. Effect of leaching time on the V leaching rate (conditions: 140 °C, 0.3 mol·L^{-1} $H_2C_2O_4$, 20 wt % H_2SO_4, 20 mL·g^{-1}).

leaching rate of V increased continuously from 83.04 to 95.65% as the leaching time increased from 3 to 7 h and stabilized after 7 h. It indicated that enough leaching time promoted the reactions between the acid solvent and spent denitration catalyst, resulting in a higher leaching rate of V. This case might be possible because sufficient time should be spent on completely released V from the spent denitration catalyst since the V-bearing lattice structure was very stable and hard to break down.[24,38] Therefore, a leaching time of 7 h was selected by considering the maximum leaching rate of 95.65%.

In summary, the optimized leaching parameters were determined to be as follows: L/S ratio of 20 mL·g^{-1}, 20 wt % sulfuric acid, and 0.3 mol·L^{-1} oxalic acid at 140 °C for 7 h. Under these conditions, the optimized V leaching rate was 95.65%. It was observed that the leaching rate of V was higher under mixed acid conditions compared to single acid conditions.[22,38]

3.3. Characterization of the Leaching Residue. The XRD diffraction patterns of the solid before and after leaching are shown in Figure 9. It can be seen that all of the diffraction peaks in both XRD patterns were matched with the standard JCPDS no. 01−84−1285 of anatase type TiO_2. It was verified that the main solid phase TiO_2 of the spent denitration catalyst had no obvious change in the leaching process.[39] After the leaching process, the support TiO_2 can be reused as a carrier to produce a new SCR catalyst.

The phase transformation of V before and after leaching was further determined by FTIR analysis.[40] In Figure 10a, the peak at 1049 cm^{-1} was attributed to characteristic of V═O while the peak at 1635 cm^{-1} was attributed to asymmetrical deformation vibrations of C═O.[41] It indicated that element V obviously existed in the solid phase before leaching. In Figure 10b, the peak of V═O at 1049 cm^{-1} disappeared while two peaks of sulfates at 1113 and 1094 cm^{-1} were generated in the solid phase after leaching.[42,43] Comparing Figure 10a,b, it

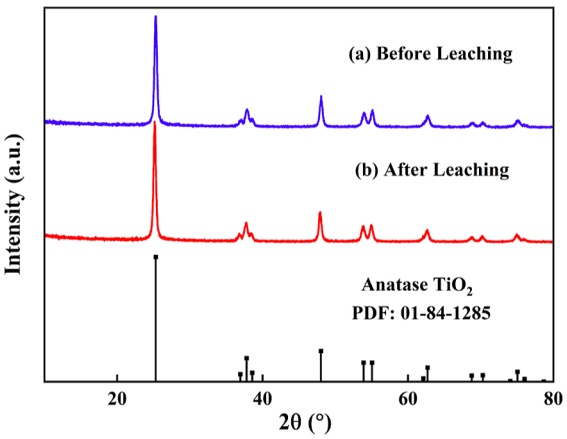

Figure 9. XRD spectra for the solid phase (a) before leaching and (b) after leaching.

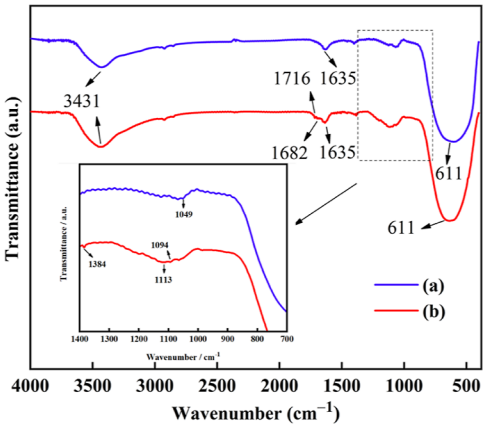

Figure 10. FTIR spectra for the solid phase (a) before leaching and (b) after leaching.

can be seen that there was no detection of V═O in the solid phase after leaching, which indicated that the V had been released from the solid phase into the leaching solvent. In addition, some sulfate precipitations might be generated during the leaching process.

3.4. Analysis of the Leaching Mechanism. As concluded from the above analysis, sulfuric acid/oxalic acid combined leaching was a complex process, and many factors influenced the leaching rate of V. Therefore, the leaching mechanism of V in this process was essentially required for the description, practical design, and operation of large-scale leaching.

3.4.1. Leaching Kinetics. As an important connection between the leaching process and mechanism, the leaching kinetics of V was studied using the shrinking core model (SCM). According to the SCM, the rate-determining step of the dissolution process could be attributed to the diffusion of materials through the solution boundary, the solid material layer, or the surface chemical reactions.[44]

The leaching kinetics of V under different temperatures were analyzed using SCM based on the solution boundary diffusion (eq 2) and surface chemical reaction (eq 3).[38,45]

$$x = k_1 t \quad (2)$$

$$1 - (1 - x)^{1/3} = k_2 t \quad (3)$$

https://doi.org/10.1021/acsomega.3c08452
ACS Omega 2024, 9, 9286−9294

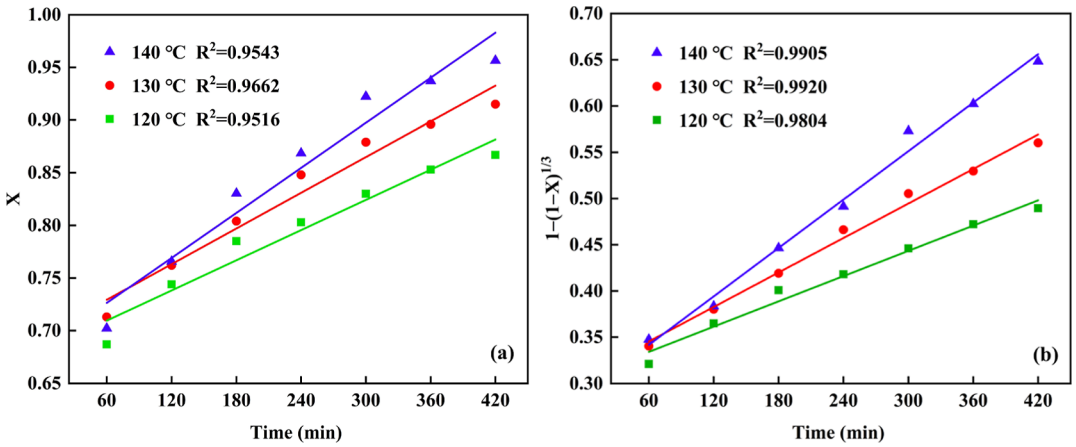

Figure 11. (a) X vs time for V and (b) $1 - (1 - X)^{1/3}$ vs time for V.

where x was the leaching rate; k_1 and k_2 were the apparent constants of different control steps, min^{-1}; and t was the leaching time, min.

Comparing Figure 11a,b, it can be seen that the latter fitting results were obviously better than the former results. The data in Figure 11b show a good linear relationship for all of the temperatures with correlation coefficients greater than 0.9804. Therefore, the leaching process was primarily controlled by the surface chemical reaction (eq 3), and the calculated rate constants (k_2) were equal to the values of the slopes. This was in accordance with the observation reported by Zhang et al. that the dissolution of V could be promoted by enhancing the surface chemical reaction.[46] Furthermore, the inhibition of the surface chemical reaction was weakened, which resulted in a faster leaching of V.

3.4.2. Chemical Reaction in the Leaching Process. As demonstrated in the above kinetics analysis, the leaching process of V with sulfuric acid/oxalic acid combined solvent was mainly controlled by the surface chemical reaction. The schematic representation of the surface chemical reaction in the leaching process that included three steps is illustrated in Figure 12.[47]

3.4.2.1. Transformation. The difficulty of releasing V from the spent denitration catalyst was determined by the interaction intensity between the leaching solvent and the mineral phases of the spent denitration catalyst.[24] In the sulfuric acid/oxalic acid combined leaching system, the crystal lattice structure of the V-bearing mineral phase was disrupted by hydrogen ions which were provided by combined acids.[20,27] In this work, the maximum concentration of hydrogen ions reached 1.99 $mol \cdot L^{-1}$, which could strongly enhance the interaction between the combined acid and the mineral phase.

From the above XPS analysis in Figure 3b, it can be seen that V existed in the forms of V(V), V(IV), and V(III) in the spent denitration catalyst. There were many different ionic species for V in the liquid phase (Table 2).[10,48] However, in a highly acidic environment such as a sulfuric acid/oxalic acid combined solvent, V(V), V(IV), and V(III) were transformed from the mineral phase into the liquid phase by the possible reactions as follows

$$V_2O_5 + 2H_3O^+ \rightarrow 2VO_2^+ + 3H_2O \quad (4)$$

$$V_2O_4 + 4H_3O^+ \rightarrow 2VO^{2+} + 6H_2O \quad (5)$$

$$V_2O_3 + 2H_3O^+ \rightarrow 2VO^+ + 3H_2O \quad (6)$$

The Gibbs free energy values of eqs 4−6 were calculated by *HSC* [enthalpy (H), entropy (S), and heat capacity (C)] chemistry thermodynamic software for verifying the possibility of the three reactions at 0−180 °C.[49,50] The calculation results are shown in Figure 13. It was found that the Gibbs free energy values of eqs 4−6 were far below zero and slightly increased as the temperature increased, indicating that all three reactions could occur spontaneously. Moreover, the spontaneous trend of the three reactions at the same temperature was arranged as (4) > (6) > (5) due to the comparison of Gibbs free energy values.

Table 2. States of V Species in Solution

existence form	V in solution
cationic species	VO^+, VO^{2+}, VO_2^+
neutral species	$VO(OH)_3$
anion species	$V_{10}O_{26}(OH)_2^{4-}$, $V_{10}O_{27}(OH)^{5-}$, $V_{10}O_{28}^{6-}$ $VO_2(OH)_2^-$, $VO_3(OH)^{2-}$, VO_4^{3-} $V_2O_6(OH)^{3-}$, $V_2O_7^{4-}$, $V_3O_9^{3-}$, $V_4O_{12}^{4-}$

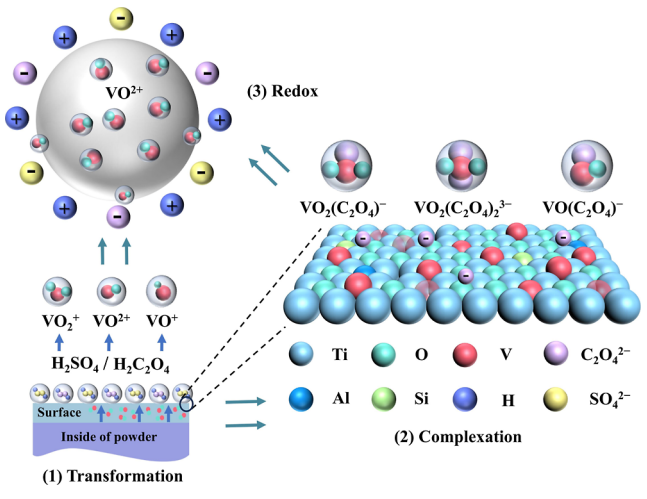

Figure 12. Chemical reaction in the leaching process.

3.4.2.2. Complexation. Oxalic acid was available to complex with metal cations due to its strong complexability.[1] The oxalate ion was a bidentate anionic ligand that could donate

https://doi.org/10.1021/acsomega.3c08452
ACS Omega 2024, 9, 9286−9294

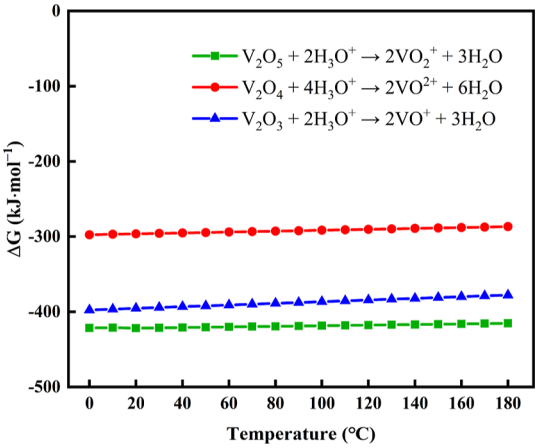

Figure 13. Gibbs free energy of eqs 4–6 at 0–180 °C.

two pairs of electrons to a metal ion.[23] This ligand was commonly known as a chelate because of its ability to attach to a metal cation in two places.[23] Most metals formed either simple oxalate compounds or oxalate complexes, or both.[28] V was reported to form only water-soluble oxalate complexes.[51]

In the soluble ions generated in the transformation mentioned above, the stable VO^{2+} ions almost no longer took part in the subsequent complexation.[22] Other soluble ions, such as VO_2^+ and VO^+, partly reacted with oxalic acid to form oxalate complexes. The related reactions are listed as follows

$$VO_2^+ + C_2O_4^{2-} \leftrightharpoons VO_2(C_2O_4)^- \quad (7)$$

$$VO_2^+ + 2HC_2O_4^- + 2H_2O \leftrightharpoons VO_2(C_2O_4)_2^{3-} + 2H_3O^+ \quad (8)$$

$$VO^+ + C_2O_4^{2-} \leftrightharpoons VO(C_2O_4)^- \quad (9)$$

3.4.2.3. Redox. The potential difference and oxidation–reduction properties of substances were employed to determine whether a redox reaction occurred or not. On the one hand, some parts of the VO_2^+ and VO^+ ions were complex with oxalic acid, while the other part of them participated in redox reactions with combined acids. This case was possible because $HC_2O_4^-$ and VO^+ had reducibility, whereas VO_2^+ had strong oxidability for its high standard redox potential of E^θ (VO_2^+/VO^{2+}) = 1.00 V, which was compared with the values E^θ (Fe^{3+}/Fe^{2+}) = 0.77 V, and even E^θ (O_2/H_2O_2) = 0.68 V.[47] Therefore, VO_2^+ rapidly reacted with VO^+ to form VO^{2+} in the combined acids with high acidity (eq 10).[10]

On the other hand, oxalate complex $VO_2(C_2O_4)^-$ formed in the above complexation further reacted with the combined acids because they were unstable and also had strong oxidability (eq 11).[52] Meanwhile, $VO(C_2O_4)^-$ could also react with $VO_2(C_2O_4)^-$ or $VO_2(C_2O_4)_2^{3-}$ due to the large potential difference between them [E^θ ($VO_2(C_2O_4)^-/VOC_2O_4$) = 1.13 V and E^θ ($VO_2(C_2O_4)_2^{3-}/VO(C_2O_4)_2^{2-}$) = 1.22 V] (eqs 12 and 13).[10]

Moreover, the redox reactions were enhanced by the large amounts of hydrogen ions from sulfuric acid.[21,27] The V existed as a stable form of VO^{2+} after the leaching process in the aqueous phase, which was in accordance with the findings reported by Al-Sheeha et al.[51] By the "complex effect" from the combined acids, the redox reactions occurring are listed as follows

$$VO_2^+ + VO^+ + HC_2O_4^- + H_3O^+ \rightarrow 2VO^{2+} + C_2O_4^{2-} + 2H_2O \quad (10)$$

$$2VO_2(C_2O_4)^- + HC_2O_4^- + 3H_3O^+ \rightarrow 2VO^{2+} + C_2O_4^{2-} + 5H_2O + 2CO_2\uparrow \quad (11)$$

$$VO_2(C_2O_4)^- + VO(C_2O_4)^- + 2H_3O^+ \rightarrow 2VO^{2+} + 2C_2O_4^{2-} + 3H_2O \quad (12)$$

$$VO_2(C_2O_4)_2^{3-} + VO(C_2O_4)^- + 2H_3O^+ \rightarrow 2VO^{2+} + 3C_2O_4^{2-} + 3H_2O \quad (13)$$

3.4.3. Verification the Valence State of V. The above analysis indicated that V existed in the form of stable VO^{2+} in the liquid phase after leaching. To verify this result, the final valence state of V in the leaching solution was further investigated by the UV–vis full spectrum scanning method (Figure 14).[53] In the experiment, the interference for detecting

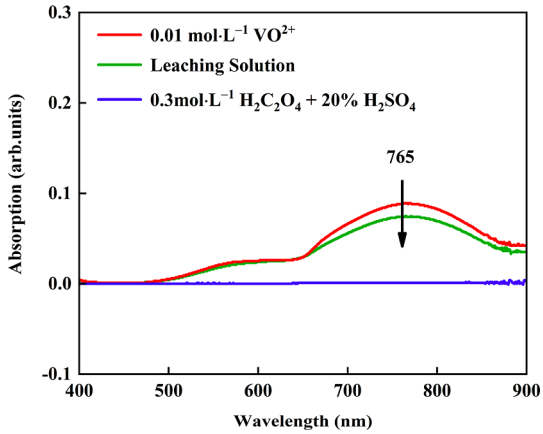

Figure 14. UV–vis spectrophotometry of V in the leaching solution.

the V valence state had been eliminated by the chosen sulfuric acid/oxalic acid combined solvent (the optimal reaction condition of 0.3 mol/L $H_2C_2O_4$ and 20 wt % H_2SO_4) as background since the leaching solution contained $C_2O_4^{2-}$ and SO_4^{2-}. Moreover, a mixture of 0.005 mol·L^{-1} VOC_2O_4 and 0.005 mol·L^{-1} $VOSO_4$ was chosen as the standard reagent for getting the most suitable absorption intensity after a series of tests.

Figure 14 shows that the valence state determination of V was not influenced by the selected background of sulfuric acid/oxalic acid combined solvent because there were no characteristic peaks of them in the scanning wavelength range. The characteristic wavelengths of V in the leach solution were consistent with those of the VOC_2O_4 /$VOSO_4$ standard reagent, with a peak at 765 nm. Hence, the final valence state of V in the leaching solution was VO^{2+}, which was consistent with the chemical reaction analysis.

4. CONCLUSIONS

V was extracted from the spent denitration catalyst using a leaching process by the sulfuric acid/oxalic acid combined solvent. Effects of several parameters on the leaching rate of V were studied first. It had been shown that the optimal leaching rate was 95.65% by 20 wt % sulfuric acid and 0.3 mol·L^{-1}

https://doi.org/10.1021/acsomega.3c08452
ACS Omega 2024, 9, 9286–9294

oxalic acid with a L/S ratio of 20 mL·g^{-1} at 140 °C for 7 h. To better describe the leaching process, the leaching kinetics of V was investigated subsequently. It was indicated that the V leaching conformed to the SCM, which meant that the surface chemical reaction played a predominant role in controlling the whole leaching process.

Moreover, the leaching mechanism of V was investigated based on the above findings. XPS analysis indicated that V primely existed in the form of V(V), V(IV), and V(III) in the spent denitration catalyst. Then, VO_2^+, VO^{2+}, and VO^+ ions formed with the transformation of V from the solid phase into the liquid phase. The transformation was highly driven by hydrogen ions providing from the sulfuric acid/oxalic acid combined solvent, which thoroughly disrupted the crystal lattice structure of the V-bearing mineral phase. Subsequently, some parts of VO_2^+ and VO^+ ions complexed with oxalic acid to form $VO_2(C_2O_4)^-$, $VO_2(C_2O_4)_2^{3-}$, and $VO(C_2O_4)^-$, whereas their other part participated in redox reactions with combined acids. Moreover, owing to the large potential difference, the ions formed in the above reactions tend to form stable VO^{2+} by redox in the strong acidic environment, which was further verified by UV−vis analysis.

In conclusion, the "complex effect" generated from the combined acids was beneficial for the transformation, complexation, and redox, thus greatly enhancing the leaching rate of V. In addition, the main solid phase TiO_2 of the spent denitration catalyst had no obvious change in the leaching process, which suggested that it was potential to prepare fresh SCR catalysts using the leaching residual as raw material. These findings could provide a new method for leaching V and pave the way for extracting other valuable metals from spent denitration catalysts.

AUTHOR INFORMATION

Corresponding Authors

Wenting Cheng − *Institute of Resources and Environmental Engineering, Shanxi University, Taiyuan 030006, China;* orcid.org/0000-0001-8624-6471; Email: wtcheng@sxu.edu.cn

Yang Li − *Longking-Coalogix Environmental Protection Technology (Shanghai) Co Ltd., Shanghai 200331, China; Jiangsu Longking-Coalogix Environmental Protection Technology Co., Ltd., Yancheng 224051, China;* Email: milestone-mater@outlook.com

Authors

Jie Li − *Institute of Resources and Environmental Engineering, Shanxi University, Taiyuan 030006, China*

Jianhang Deng − *Shanghai Shangde Experimental School Noble Academy, Shanghai 201315, China*

Fangqin Cheng − *Institute of Resources and Environmental Engineering, Shanxi University, Taiyuan 030006, China;* orcid.org/0000-0002-2961-2989

Complete contact information is available at: https://pubs.acs.org/10.1021/acsomega.3c08452

Notes

The authors declare no competing financial interest.

ACKNOWLEDGMENTS

The support of National Energy-Saving and Low-Carbon Materials Production and Application Demonstration Platform Program (no. TC220H06N) is gratefully acknowledged.

REFERENCES

(1) Zhang, Q.; Wu, Y.; Yuan, H. Recycling strategies of spent V_2O_5-WO_3/TiO_2 catalyst: A review. *Resour. Conserv. Recycl.* **2020**, *161*, 104983.

(2) Wu, Z.; Chen, H.; Wan, Z.; Zhang, S.; Zeng, Y.; Guo, H.; Zhong, Q.; Li, X.; Han, J.; Rong, W. Promotional Effect of S Doping on V_2O_5-WO_3/TiO_2 Catalysts for Low-Temperature NOx Reduction with NH_3. *Ind. Eng. Chem. Res.* **2020**, *59* (35), 15478−15488.

(3) Yin, Y.; Li, X.; Li, K.; Liu, R.; Wu, H.; Zhu, T. Formic Acid-Mediated Regeneration Strategy for As-Poisoned V_2O_5-WO_3/TiO_2 Catalysts with Lossless Catalytic Activity and Simultaneous As Recycling. *Environ. Sci. Technol.* **2022**, *56* (17), 12625−12634.

(4) Lanza, A.; Usberti, N.; Forzatti, P.; Beretta, A. Kinetic and Mass Transfer Effects of Fly Ash Deposition on the Performance of SCR Monoliths: A Study in Microslab Reactor. *Ind. Eng. Chem. Res.* **2021**, *60* (18), 6742−6752.

(5) Wen, C.; Guo, Y.; Yan, K.; Zhang, H. Variations in the physicochemical properties of spent honeycomb V_2O_5-WO_3/TiO_2 catalysts from PC and CFB boilers SCR denitration systems. *Fuel* **2023**, *347*, 128384.

(6) Deng, L.; Zhu, Z.; Wang, Y.; Ma, S.; Zhang, Y.; Zhang, T.; Hu, Z.; Che, D. Deactivation Influence of HF on the V_2O_5-WO_3-TiO_2 SCR Catalyst. *Energy Fuels* **2021**, *35* (5), 4377−4386.

(7) Wang, B.; Liu, Z.; Lin, D.; Cao, Z.; He, F.; Lu, G.; Xiao, Y. A Review on Recovery and Utilization of Spent V_2O_5-WO_3/TiO_2 Catalyst. *Mater. Rev.* **2021**, *35*, 15001−15010.

(8) Chen, C.; Liang, Y.; Tang, Q.; Li, D.; Liu, L.; Dong, J. *In Situ* Growth of Tungsten Oxide on Alumina to Boost the Catalytic Performance of Platinum for Glycerol Hydrogenolysis. *Ind. Eng. Chem. Res.* **2022**, *61* (34), 12504−12512.

(9) Qian, L.; Yang, T.; Long, H.; Ding, L.; Xu, C. C. Recycling of Waste V_2O_5-WO_3/TiO_2 Catalysts in the Iron Ore Sintering Process Via a Preballing Approach. *ACS Sustain. Chem. Eng.* **2021**, *9* (48), 16373−16383.

(10) Hu, P.; Hu, P.; Vu, T. D.; Li, M.; Wang, S.; Ke, Y.; Zeng, X.; Mai, L.; Long, Y. Vanadium Oxide: Phase Diagrams,Structures,Synthesis, and Applications. *Chem. Rev.* **2023**, *123* (8), 4353−4415.

(11) Bai, X.; Shang, X.; Wan, H.; Che, Y.; Yang, B.; He, J.; Song, J. Sustainable recycling of titanium from TiO_2 in spent SCR denitration catalyst via molten salt electrolysis. *J. Energy Chem.* **2021**, *58*, 557−563.

(12) Yang, B.; Zhou, J.; Wang, W.; Liu, C.; Zhou, D.; Yang, L. Extraction and separation of tungsten and vanadium from spent V_2O_5-WO_3/TiO_2 SCR catalysts and recovery of TiO_2 and sodium titanate nanorods as adsorbent for heavy metal ions. *Colloids Surf., A* **2020**, *601*, 124963.

(13) Nie, Z.; Ma, L.; Xi, X.; Guo, F.; Nie, Z. Studying the leaching mechanism of spent SCR catalyst with different leaching agents (NaOH, H_2SO_4, HCl and HNO_3) using DFT calculations. *Appl. Surf. Sci.* **2022**, *584*, 152577.

(14) Wei, Y.; Li, D.; Qiao, J.; Guo, X. Recovery of spent SCR denitration catalyst: A review and recent advances. *J. Environ. Chem. Eng.* **2023**, *11* (3), 110104.

(15) Wang, L.; Qing, M.; Yang, X.; Su, S.; Wang, Z.; Li, H.; Liu, L.; Wang, Y.; Hu, S.; Xiang, J. Solidification and Leaching Behaviors of V and As in a Spent Catalyst-Containing Concrete. *Energy Fuels* **2020**, *34* (6), 7209−7217.

(16) Ding, Y.; Zhang, S.; Liu, B.; Zheng, H.; Chang, C.-c.; Ekberg, C. Recovery of precious metals from electronic waste and spent catalysts: A review. *Resour. Conserv. Recycl.* **2019**, *141*, 284−298.

(17) Gao, W.; Liu, C.; Cao, H.; Zheng, X.; Lin, X.; Wang, H.; Zhang, Y.; Sun, Z. Comprehensive evaluation on effective leaching of critical metals from spent lithium-ion batteries. *Waste Manag.* **2018**, *75*, 477−485.

(18) Chen, X.; Lan, X.; Zhang, Q.; Ma, H.; Zhou, J. Leaching vanadium by high concentration sulfuric acid from stone coal. *Trans. Nonferrous Met. Soc. China* **2010**, *20*, 123−126.

(19) Erust, C.; Akcil, A.; Bedelova, Z.; Anarbekov, K.; Baikonurova, A.; Tuncuk, A. Recovery of vanadium from spent catalysts of sulfuric

acid plant by using inorganic and organic acids: Laboratory and semi-pilot tests. *Waste Manag.* **2016**, *49*, 455−461.
(20) Yao, Y.; Zhu, M.; Zhao, Z.; Tong, B.; Fan, Y.; Hua, Z. Hydrometallurgical Processes for Recycling Spent Lithium-Ion Batteries: A Critical Review. *ACS Sustain. Chem. Eng.* **2018**, *6* (11), 13611−13627.
(21) Hu, P.; Zhang, Y.; Huang, J.; Liu, T.; Yuan, Y.; Xue, N. Eco-Friendly Leaching and Separation of Vanadium over Iron Impurity from Vanadium-Bearing Shale Using Oxalic Acid as a Leachant. *ACS Sustain. Chem. Eng.* **2018**, *6* (2), 1900−1908.
(22) Wu, W.; Wang, C.; Bao, W.; Li, H. Selective reduction leaching of vanadium and iron by oxalic acid from spent V_2O_5-WO_3/TiO_2 catalyst. *Hydrometallurgy* **2018**, *179*, 52−59.
(23) Verma, A.; Kore, R.; Corbin, D. R.; Shiflett, M. B. Metal Recovery Using Oxalate Chemistry: A Technical Review. *Ind. Eng. Chem. Res.* **2019**, *58* (34), 15381−15393.
(24) Shekhar Samanta, N.; Das, P. P.; Dhara, S.; Purkait, M. K. An Overview of Precious Metal Recovery from Steel Industry Slag: Recovery Strategy and Utilization. *Ind. Eng. Chem. Res.* **2023**, *62* (23), 9006−9031.
(25) Liu, J.; Wang, C.; Wang, X.; Li, H.; Zhao, C. Iron removal and titanium dioxide support recovery from spent V_2O_5-WO_3/TiO_2 catalyst. *Sep. Purif. Technol.* **2022**, *301*, 121934.
(26) Wang, B.; Yang, Q. Recovery of V_2O_5 from spent SCR catalyst by H_2SO_4-ascorbic acid leaching and chemical precipitation. *J. Environ. Chem. Eng.* **2022**, *10* (6), 108719.
(27) Li, P.; Luo, S.-H.; Su, F.; Zhang, L.; Yan, S.; Lei, X.; Mu, W.; Wang, Q.; Zhang, Y.; Liu, X.; Hou, P. Optimization of Synergistic Leaching of Valuable Metals from Spent Lithium-Ion Batteries by the Sulfuric Acid-Malonic Acid System Using Response Surface Methodology. *ACS Appl. Mater. Interfaces* **2022**, *14* (9), 11359−11374.
(28) Wu, W.; Wang, C.; Wang, X.; Li, H. Removal of Vand Fe from spent denitrification catalyst by using oxalic acid: Study of dissolution kinetics and toxicity. *Green Energy Environ.* **2021**, *6* (5), 660−669.
(29) Liu, Q.; Quan, S.; Liu, Z.; Liu, Q. Leaching of vanadium and tungsten from spent V_2O_5-WO_3/TiO_2 catalyst by ionic liquids. *Hydrometallurgy* **2022**, *213*, 105938.
(30) Ferella, F. A review on management and recycling of spent selective catalytic reduction catalysts. *J. Cleaner Prod.* **2020**, *246*, 118990.
(31) Shi, Q.; Du, X.; Wang, X.; Yang, G.; Wan, Y.; Chen, Y.; Song, L.; Xue, Z.; Zhang, L. Recycling of Waste SCR Catalysts Using a Catalytic Filter: A Study on the Catalytic Performance for NOx Abatement. *Ind. Eng. Chem. Res.* **2021**, *60* (12), 4622−4629.
(32) Guan, B.; Chen, J.; Guo, J.; Liu, Z.; Zheng, C.; Zhou, J.; Su, T.; Zhang, Y.; Yuan, Y.; Dang, H.; Xu, B.; Xu, C.; Zeng, W.; Huang, Z. Study on Effect and Mechanism of Alkaline Earth Metal Poisoning on Cu/SSZ-13 Catalysts for Selective Catalytic Reduction of NOx with NH_3. *Ind. Eng. Chem. Res.* **2023**, *62* (25), 9662−9672.
(33) Zhang, Q.; Wu, Y.; Li, L.; Zuo, T. Sustainable Approach for Spent V_2O_5-WO_3/TiO_2 Catalysts Management: Selective Recovery of Heavy Metal Vanadium and Production of Value-Added WO_3-TiO_2 Photocatalysts. *ACS Sustain. Chem. Eng.* **2018**, *6* (9), 12502−12510.
(34) Xue, Y.; Zhang, Y.; Zhang, Y.; Zheng, S.; Zhang, Y.; Jin, W. Electrochemical detoxification and recovery of spent SCR catalyst by in-situ generated reactive oxygen species in alkaline media. *Chem. Eng. J.* **2017**, *325*, 544−553.
(35) Gan, L.; Chen, J.; Peng, Y.; Yu, J.; Tran, T.; Li, K.; Wang, D.; Xu, G.; Li, J. NOx Removal over V_2O_5/WO_3-TiO_2 Prepared by a Grinding Method: Influence of the Precursor on Vanadium Dispersion. *Ind. Eng. Chem. Res.* **2018**, *57* (1), 150−157.
(36) Li, P.; Luo, S.-H.; Feng, J.; Lv, F.; Yan, S.; Wang, Q.; Zhang, Y.; Mu, W.; Liu, X.; Lei, X.; Teng, F.; Li, X.; Chang, L.-j.; Liang, J.; et al. Study on the high-efficiency separation of Fe in extracted vanadium residue by sulfuric acid roasting and the solidification behavior of V and Cr. *Sep. Purif. Technol.* **2021**, *269*, 118687.
(37) Cao, Y.; Yuan, J.; Du, H.; Dreisinger, D.; Li, M. A clean and efficient approach for recovery of vanadium and tungsten from spent SCR catalyst. *Miner. Eng.* **2021**, *165*, 106857.
(38) Li, Q.; Liu, Z.; Liu, Q. Kinetics of Vanadium Leaching from a Spent Industrial V_2O_5/TiO_2 Catalyst by Sulfuric Acid. *Ind. Eng. Chem. Res.* **2014**, *53* (8), 2956−2962.
(39) Niu, J.; Jia, J.; Zhang, H.; Guo, Y.; Li, L.; Cheng, F. Insights on the dual role of low-rank coal with high mineral catalysis index (LRC-HMCI) during blending coal for activated carbon production and low-temperature NH_3-SCR of NO. *Fuel* **2023**, *349*, 128591.
(40) Yang, B.; Mu, W.; Woon Lo, B. T.; Liu, S.; Chen, Z.; France, L. J.; Li, X. Efficient TiO_2-Nanobelt-Supported Ir Catalysts for FCC-Generated NOx and CO Remediation. *Ind. Eng. Chem. Res.* **2020**, *59* (20), 9655−9665.
(41) Shang, X.; Hu, G.; He, C.; Zhao, J.; Zhang, F.; Xu, Y.; Zhang, Y.; Li, J.; Chen, J. Regeneration of full-scale commercial honeycomb monolith catalyst (V_2O_5-WO_3/TiO_2) used in coal-fired power plant. *J. Ind. Eng. Chem.* **2012**, *18* (1), 513−519.
(42) Liu, Z.; Huang, J.; Zhang, Y.; Liu, T.; Hu, P.; Liu, H.; Zheng, Q. Separation and recovery of iron impurities from a complex oxalic acid solution containing vanadium by $K_3Fe(C_2O_4)_3$ center dot $3H_2O$ crystallization. *Sep. Purif. Technol.* **2020**, *232*, 115970.
(43) Zeng, Y.; Zhao, J.; Wang, S.; Ren, X.; Tan, Y.; Lu, Y.-R.; Xi, S.; Wang, J.; Jaouen, F.; Li, X.; Huang, Y.; Zhang, T.; Liu, B. Unraveling the Electronic Structure and Dynamics of the Atomically Dispersed Iron Sites in Electrochemical CO_2 Reduction. *J. Am. Chem. Soc.* **2023**, *145* (28), 15600−15610.
(44) Li, Z.; He, L.; Zhu, Y.; Yang, C. A Green and Cost-Effective Method for Production of LiOH from Spent $LiFePO_4$. *ACS Sustain. Chem. Eng.* **2020**, *8* (42), 15915−15926.
(45) Li, W.; Yan, X.; Niu, Z.; Zhu, X. Selective recovery of vanadium from red mud by leaching with using oxalic acid and sodium sulfite. *J. Environ. Chem. Eng.* **2021**, *9* (4), 105669.
(46) Zhang, C.; Min, X. B.; Zhang, J. Q.; Wang, M.; Li, Y. C.; Fei, J. C. Reductive clean leaching process of cadmium from hydrometallurgical zinc neutral leaching residue using sulfur dioxide. *J. Cleaner Prod.* **2016**, *113*, 910−918.
(47) Wachs, I. E. Catalysis science of supported vanadium oxide catalysts. *Dalton Trans.* **2013**, *42* (33), 11762−11769.
(48) Li, W.; Zhang, Y. M.; Liu, T.; Huang, J.; Wang, Y. Comparison of ion exchange and solvent extraction in recovering vanadium from sulfuric acid leach solutions of stone coal. *Hydrometallurgy* **2013**, *131*−*132*, 1−7.
(49) Jeon, M. K.; Shin, J. M.; Park, J. J.; Park, G. I. Simulation of Cs behavior during the high temperature voloxidation process using the HSC chemistry code. *J. Nucl. Mater.* **2012**, *430* (1−3), 37−43.
(50) Walle, E. v.; Perrot, P.; Foct, J.; Parise, M. Evaluation of the Cs-Mo-I-O and Cs-U-I-O diagrams and determination of iodine and oxygen partial pressure in spent nuclear fuel rods. *J. Phys. Chem. Solids* **2005**, *66*, 655−664.
(51) Al-Sheeha, H.; Marafi, M.; Raghavan, V.; Rana, M. S. Recycling and Recovery Routes for Spent Hydroprocessing Catalyst Waste. *Ind. Eng. Chem. Res.* **2013**, *52* (36), 12794−12801.
(52) Bruyere, V. I. E.; García Rodenas, L. A.; Morando, P. J.; Blesa, M. A. Reduction of vanadium(v) by oxalic acid in aqueous acid solutions. *J. Chem. Soc. Dalton Trans.* **2001**, 3593−3597.
(53) Chen, F.-Y.; Chen, H.; Hou, S.-Y.; Liu, J.; Yan, C. Spectrophotometry Analysis of Different Valence State of Vanadium in Vanadium Battery Electrolyte. *Spectrosc. Spectr. Anal.* **2011**, *31* (10), 2839−2842.

https://doi.org/10.1021/acsomega.3c08452
ACS Omega 2024, 9, 9286−9294